

Manual for DFT+ GW +BSE and the related matters

Jinyuan Wu

January 14, 2023

Chapter 1

GW and BSE

1.1 Preliminaries

1.1.1 Details in diagrammatics

This section briefly goes through some tricky aspects of Feynman diagram techniques that may seem puzzling when we do concrete calculations.

1.1.1.1 Infinitesimals

Note that here we need to add some convergence factors. The first is about the value of the propagator to ensure that when $t = 0$, $\mathcal{T} \langle c(t)c^\dagger(0) \rangle$ is the particle number (so that if we evaluate the tadpole diagram, we get the Hartree term), the contribution of an electron line is actually

$$\begin{aligned} \mathcal{T} \langle c_{\mathbf{k}}(t)c_{\mathbf{k}}^\dagger(0) \rangle &:= \mathcal{T} \langle c_{\mathbf{k}}(t-0^+)c_{\mathbf{k}}^\dagger(0) \rangle \\ &= \int \frac{d\omega}{2\pi} e^{-i\omega(t-0^+)} \underbrace{\frac{i}{\omega - \xi_{\mathbf{k}} + i0^+ \operatorname{sgn}(\xi_{\mathbf{k}})}}_{iG_0(\omega, \mathbf{k})} = \int \frac{d\omega}{2\pi} e^{-i\omega t} e^{i\omega 0^+} iG_0(\omega, \mathbf{k}). \end{aligned} \quad (1.1)$$

The necessity of this $e^{i\omega 0^+}$ factor can also be seen by explicitly doing the integration: when $t = 0$, if we ignore the $e^{i\omega 0^+}$ factor, we get

$$\int \frac{d\omega}{2\pi} \frac{i}{\omega - \xi_{\mathbf{k}} + i0^+ \operatorname{sgn}(\xi_{\mathbf{k}})}.$$

This integral is not zero, but we want it to be zero when $\xi_{\mathbf{k}} > 0$, so we have to add a $e^{i\omega 0^+}$ factor to make the integrand approaches zero quickly enough in the upper plane, so we can construct an integration contour in the upper plane, in which there is no pole, and

$$\int_{|\omega|=R \gg 1} \frac{d\omega}{2\pi} \frac{i}{\omega - \xi_{\mathbf{k}} + i0^+ \operatorname{sgn}(\xi_{\mathbf{k}})} = 0.$$

Another mini-regularization is when necessary, for a real space interaction line – screened or unscreened – we should assume the “out-time” is the “in-time” plus 0^+ , because the Coulomb interaction isn’t really spontaneous and there is a small time retardation. In the frequency space, we need to assume that there is an infinite amount of energy on the interaction line,

For bare Coulomb interaction this is rarely needed, because we don’t have ω dependence in the potential, and it makes no sense to discuss the poles when we change ω . It does make sense to talk about retardation in the relativistic origin of Coulomb interaction: the Coulomb interaction is mediated by virtual photons, and is therefore proportional to the off-shell (i.e. $\omega \rightarrow 0$) limit of the photon propagator, which has $\omega^2 - \mathbf{q}^2 + i0^+$ as the denominator, and we get

$$V(q) = \frac{4\pi e^2}{\mathbf{q}^2 - \omega^2 - i0^+}. \quad (1.2)$$

For screened Coulomb interaction, however, the correct retardation is important, because now something looking like (1.2) appears again.

1.1.1.2 The position of imaginary units

In this section I only consider how many imaginary units there are in front of Green functions, self energies, etc. Normalization factors like 2π or V involved in summation of \mathbf{r} or \mathbf{k} are not considered.

The self-energy correction is visualized as the follows:

$$\text{double line with arrow} = \text{single line with arrow} + \text{single line with arrow through loop} \quad (1.3)$$

and from it we have

$$iG = iG_0 + iG_0 iG \times \text{loop} \quad .$$

It's then a good idea to define

$$-i\Sigma = \text{loop} \quad , \quad (1.4)$$

because in this case, we have

$$G = G_0 + GG_0\Sigma, \quad (1.5)$$

and therefore

$$\underbrace{\omega - \xi_{\mathbf{k}}^0}_{1/G_0} = \underbrace{\omega - \xi_{\mathbf{k}}}_{1/G} + \Sigma, \quad (1.6)$$

which agrees with the definition of the self energy as the shift of single-particle energy from the free dispersion.

Similarly, we define the corrected interaction line as

$$-iW = \text{wavy line} \quad , \quad (1.7)$$

because in this way, when there is no interaction corrections, we have

$$W = \frac{e^2}{r} =: v. \quad (1.8)$$

1.1.1.3 About “antiparticles”

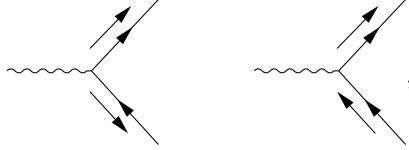
The directions of momentum lines indicate whether the particles are created or annihilated. When the momentum arrow goes against the arrow on a line, we say this line is an antiparticle line. But here is a puzzle: we know there is no such thing as positrons in condensed matter physics, so what does “antiparticle” mean?

Here the problem lies on what it means to be the antiparticle of a kind of particle. In particle physics, when we do the particle-antiparticle transformation to an electron state whose polarization is one of the Dirac basis, a ψ^+ particle is flipped into a ψ^- particle and vice versa. In condensed matter physics, the label of ψ^+ and ψ^- (or ϕ and χ as people often call them:

$\psi = (\phi, \chi)$ is no longer there: the χ modes in the Dirac field have already been integrated out. So electrons in condensed matter physics don't really have antiparticles in the context of high energy physics.

Indeed, if we are still dealing with scattering problems in the non-relativistic limit, the antiparticle lines don't appear at all! And similar to the case in QED (which can be checked in Peskin (A.6)), no separate momentum arrows parallel to the internal lines are needed: When calculating the propagator, the processes of both “an electron traveling forward” and “a hole traveling backward” are automatically covered together.

The antiparticle lines only appear when there are electrons in the ground state, which usually indicates there is a $-\mu N$ term in the Hamiltonian so having some preexisting electrons lower the energy further, and this differs with the scattering case only in the rules pertaining to the external lines. For external lines, we now have diagrams like the following:



because now it's possible to annihilate a preexisting electron in the ground state, but for internal lines, momentum labels can still be directly attached to the internal lines. This can be also seen by reckoning how Feynman rules are derived: the series we obtain by expanding e^{-iHt} contains field operators, not single creation or annihilation operators, and after Wick expansion, the correlation functions we get are all like $\langle \bar{\psi}\psi \rangle$, and of course an annihilation operator appearing in the expression of the out state in terms of the ground state can be contracted with a creative operator in e^{-iHt} , and this is visualized as an “antiparticle” external line with an outward momentum line. So here, the “particle-antiparticle transformation” is just swapping $c_{\mathbf{k}}$ and $c_{\mathbf{k}}^\dagger$ – this operation is still legit in condensed matter physics, because it doesn't involve the χ field; of course, the operation doesn't create that kind of antiparticle in high energy physics.

No real modification happens to the propagator when there are electrons in the ground state. We have

$$\int_{-\infty}^{\infty} e^{i\omega t} dt \mathcal{T} \langle c_{\mathbf{k}}(t) c_{\mathbf{k}}^\dagger(0) \rangle = \frac{i}{\omega - \epsilon_{\mathbf{k}} + \mu}, \quad (1.9)$$

which can be straightforwardly obtained by looking at

$$H = \sum_{\mathbf{k}} \epsilon_{\mathbf{k}} c_{\mathbf{k}}^\dagger c_{\mathbf{k}} - \mu N \quad (1.10)$$

without doing any calculation.

Now we have to face the tough question: if antiparticle lines are there when there is a Fermi ball in the ground state, then why poles corresponding to antiparticles (whatever they are) are absent in the propagator? The answer is, for a \mathbf{k} on an antiparticle line appearing in diagrams, the corresponding pole can indeed be understood as a pole of an antiparticle: for an antiparticle line with momentum \mathbf{k} , \mathbf{k} has to be under the Fermi surface in the ground state, so $\omega_{\mathbf{k}} = \epsilon_{\mathbf{k}} - \mu < 0$, and the point $\omega = \omega_{\mathbf{k}}$ thus may be understood as an antiparticle pole. But here is a rather strong antisymmetry between particles and antiparticles: in external lines, when particles appear (\mathbf{k} over Fermi surface), antiparticles never appear; when antiparticles appear (\mathbf{k} below Fermi surface), particles never appear. The spectrum of electrons is split into two halves: for the part over the Fermi surface, only particles are visible, while for the part below the Fermi surface, only antiparticles are visible.

This means we can do away with antiparticle lines. By defining

$$b_{\mathbf{k}} = \begin{cases} c_{\mathbf{k}}, & \epsilon_{\mathbf{k}} > \mu, \\ c_{\mathbf{k}}^\dagger, & \epsilon_{\mathbf{k}} < \mu, \end{cases} \quad (1.11)$$

for $\epsilon_{\mathbf{k}} < \mu$, we have

$$\int_{-\infty}^{\infty} e^{i\omega t} dt \mathcal{T} \langle b_{\mathbf{k}}(t) b_{\mathbf{k}}^\dagger(0) \rangle = \frac{i}{\omega - \mu + \epsilon_{\mathbf{k}}}, \quad (1.12)$$

and now all poles have positive energies. It's also easy to replace c operators in all interaction vertices with b operators, so now, in the theory in terms of b operators, there is no antiparticle poles or Feynman diagrammatic antiparticle lines. Indeed, b operators give the true free excitation spectrum in a system with a non-zero chemical potential.

For $\epsilon_{\mathbf{k}} < \mu$, $b_{\mathbf{k}}^\dagger$ is said to *create* a **hole**. The energy of a hole is still positive: the energy of a state with a hole with momentum \mathbf{k} is

$$\sum_{\mathbf{k}' \neq \mathbf{k}, \epsilon_{\mathbf{k}'} < \mu} \epsilon_{\mathbf{k}'} - \mu(N-1),$$

and compared with the ground state, the energy of the hole is

$$\begin{aligned} E &= \sum_{\mathbf{k}' \neq \mathbf{k}, \epsilon_{\mathbf{k}'} < \mu} \epsilon_{\mathbf{k}'} - \mu(N-1) - \left(\sum_{\epsilon_{\mathbf{k}'} < \mu} \epsilon_{\mathbf{k}'} - \mu N \right) \\ &= \mu - \epsilon_{\mathbf{k}} > 0. \end{aligned} \tag{1.13}$$

So, we may say a hole is the antiparticle of an electron, but when we talk about the former, the latter is just a part of the background. Unlike the case in particle physics, where the electron and the positron are definitely two things, the hole and the electron are basically two *representations* of the *same* thing. (But this doesn't make talking about "annihilation between an electron and a hole" nonsense, because in an annihilation-between-electron-and-hole process, the n and \mathbf{k} numbers of the electron and the hole are different, so there is no problem of double counting the same mode in two representations, etc.)

1.1.1.4 Normalization

$$\int_{-\infty}^{\infty} e^{i\omega t} dt \tag{1.14}$$

1.1.2 Feynman rules for actual calculation

1.1.2.1 In the free space

TODO: n interaction line $\Rightarrow n$ independent momenta, not all of which are on Coulomb interaction lines

A large benefit of this formalism is it lifts the burden to worry about normalization concerning δ -functions: no δ -function appears in the rules now!

$$v(\mathbf{q}) = \frac{4\pi e^2}{q^2}. \tag{1.15}$$

1.1.2.2 In a crystal

There are several things that need attention concerning Feynman rules in condensed physics:

- The propagator is no longer $1/(\omega - \mathbf{k}^2/2m)$, but $\propto \sum_{\mathbf{k}} \psi_{n\mathbf{k}}(\mathbf{r}) \psi_{n\mathbf{k}}^*(\mathbf{r}') / (\omega - \xi_{n\mathbf{k}})$;
- The crystal momentum \mathbf{k} appears above. To carry out Feynman diagrammatic calculations in an actual computer, a cutoff on the density of \mathbf{k} points is needed (essentially, a cutoff on the size of the system V). This means we should replace $\int d^3\mathbf{k}/2\pi$ with properly normalized $\sum_{\mathbf{k}}$, where \mathbf{k} goes over the discretely infinite \mathbf{k} -grid.
- Usually we limit all momenta to the **first Brillouin zone (1BZ)**, and therefore a sum over an unbounded momentum variable \mathbf{k} or \mathbf{q} has to be recast into $\sum_{\mathbf{G}} \sum_{\mathbf{k}} f(\mathbf{k} + \mathbf{G})$.

Below I describe a set of Feynman rules that are compatible with the notation in [7]. Note that there is no controversy over normalization in the *real space* Feynman diagrams: although the inner structure of $G(1,2)$ has changed in the presence of the crystal potential, its relation with other diagrammatic components as abstract entities is never changed. Thus, starting from the space-in-real-space-and-time-in-frequency-space formalism may be a good idea: the free-space momentum formalism however is an important reference for normalization constants. In the

space-in-real-space-and-time-in-frequency-space formalism, in a diagram containing n Coulomb interaction lines, the variables summed over are n frequency variables, and $2n$ space variables, and we just need to do

$$\int \frac{d\omega_1}{2\pi} \dots \int \frac{d\omega_n}{2\pi} \int d^3\mathbf{r}_1 \dots \int d^3\mathbf{r}_{2n}. \quad (1.16)$$

We choose a normalization scheme for $\psi_{n\mathbf{k}}$ such that

$$c_{n\mathbf{k}}^\dagger = \int d^3\mathbf{r} \underbrace{e^{i\mathbf{k}\cdot\mathbf{r}} u_{n\mathbf{k}}(\mathbf{r})}_{\psi_{n\mathbf{k}}} \psi^\dagger(\mathbf{r}), \quad \{c_{n\mathbf{k}}, c_{n'\mathbf{k}'}^\dagger\} = \delta_{nn'} \delta_{\mathbf{k}\mathbf{k}'}, \quad (1.17)$$

where $\psi^\dagger(\mathbf{r})$ is the complex conjugate of the non-relativistic electron field operator. This leads to the normalization condition

$$\int d^3\mathbf{r} \psi_{n\mathbf{k}}^*(\mathbf{r}) \psi_{n'\mathbf{k}'}(\mathbf{r}) = \delta_{nn'} \delta_{\mathbf{k}\mathbf{k}'}, \quad (1.18)$$

and

$$G^0(\mathbf{r}, \mathbf{r}', \omega) = \sum_{n, \mathbf{k}} \frac{\psi_{n\mathbf{k}}(\mathbf{r}) \psi_{n\mathbf{k}}^*(\mathbf{r}')}{\omega - \xi_{n\mathbf{k}} + i0^+ \text{sgn}(\omega)}. \quad (1.19)$$

In the free-electron case, we expect

$$\psi_{n\mathbf{k}}(\mathbf{r}) = \frac{1}{\sqrt{V}} e^{i(\mathbf{k} + \mathbf{G}_n) \cdot \mathbf{r}}, \quad (1.20)$$

and therefore (note that the only possibility for $\mathbf{G}_n + \mathbf{k}$ to be equal to $\mathbf{G}_{n'} + \mathbf{k}'$ is for \mathbf{G}_n to be $\mathbf{G}_{n'}$ and \mathbf{k} to be \mathbf{k}')

$$\text{LHS of (1.18)} = \frac{1}{V} \int d^3\mathbf{r} e^{i\mathbf{r} \cdot (-\mathbf{G}_n - \mathbf{k} + \mathbf{G}_{n'} + \mathbf{k}')} = \frac{1}{V} V \delta_{\mathbf{G}_n + \mathbf{k}, \mathbf{G}_{n'} + \mathbf{k}'} = \delta_{nn'} \delta_{\mathbf{k}\mathbf{k}'},$$

and

$$\begin{aligned} \text{RHS of (1.19)} &= \frac{1}{V} \sum_{n, \mathbf{k}} e^{i(\mathbf{k} + \mathbf{G}_n) \cdot (\mathbf{r} - \mathbf{r}')} = \frac{1}{V} \sum_{\text{unbounded } \mathbf{k}} e^{i\mathbf{k} \cdot (\mathbf{r} - \mathbf{r}')} \\ &= \int \frac{d^3\mathbf{k}}{(2\pi)^3} e^{i\mathbf{k} \cdot (\mathbf{r} - \mathbf{r}')} =: \text{LHS of (1.19)}, \end{aligned}$$

so (1.18) and (1.19) go back to the free-space case.

Now we consider what happens when we encounter a Coulomb interaction line. The structure in which a Coulomb interaction line is connected to four electron lines gives rise to the following factor in the interpretation of the diagram:

$$M = \int d^3\mathbf{r} \int d^3\mathbf{r}' iG(\mathbf{r}_4, \mathbf{r}, \omega_1) iG(\mathbf{r}_3, \mathbf{r}', \omega_2) iG(\mathbf{r}', \mathbf{r}_2, \omega_3) iG(\mathbf{r}, \mathbf{r}_1, \omega_4) (-i)v(\mathbf{r} - \mathbf{r}'). \quad (1.21)$$

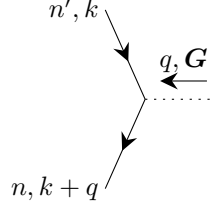
Note that here ω_4 is just a shorthand of $\omega_1 + \omega_2 - \omega_3$ and this condition is *not* imposed by a δ -function factor according to the rules listed above for the free-space case (if we want to make this expression really symmetric, we should add a $2\pi\delta(\sum \omega)$ factor, and let, say, $\int d\omega_4/2\pi$ explicitly impose the energy conservation condition for us). Inserting (1.19) into the above expression, and using the definition

$$v(\mathbf{r} - \mathbf{r}') = \int \frac{d^3\mathbf{p}}{(2\pi)^3} e^{i\mathbf{p} \cdot (\mathbf{r} - \mathbf{r}')} v(\mathbf{p}), \quad (1.22)$$

we have

$$\begin{aligned} M &= \psi_4(\mathbf{r}_4) \psi_3(\mathbf{r}_3) \psi_2^*(\mathbf{r}_2) \psi_1^*(\mathbf{r}_1) \\ &\times \int \frac{d^3\mathbf{q}}{(2\pi)^3} \sum_{1,2,3,4} \frac{i}{\omega_1 - \xi_4 + i0^+ \text{sgn}(\omega_1)} \frac{i}{\omega_1 - \xi_3 + i0^+ \text{sgn}(\omega_2)} \\ &\times \frac{i}{\omega_1 - \xi_2 + i0^+ \text{sgn}(\omega_3)} \frac{i}{\omega_1 - \xi_1 + i0^+ \text{sgn}(\omega_4)} \\ &\times \int d^3\mathbf{r} \psi_4^*(\mathbf{r}) \psi_1(\mathbf{r}) e^{i\mathbf{q} \cdot \mathbf{r}} \int d^3\mathbf{r}' \psi_3^*(\mathbf{r}') \psi_2(\mathbf{r}') e^{-i\mathbf{q} \cdot \mathbf{r}'} v(\mathbf{q}), \end{aligned} \quad (1.23)$$

and



$$= \langle n, \mathbf{k} + \mathbf{q} | e^{i(\mathbf{q} + \mathbf{G}) \cdot \mathbf{r}} | n' \mathbf{k} \rangle. \quad (1.28)$$

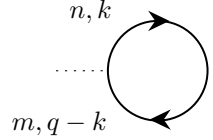
The sign is decided by the direction of \mathbf{q} . The direction of \mathbf{q} doesn't matter: we *don't* sum over the two directions. The value of \mathbf{q} is determined by the values of free momentum variables; if \mathbf{q} is not selected as a free momentum variable, it shouldn't be integrated over.

Now we compare the above Feynman rules with the momentum space Feynman rules in Section 1.1.2.1. Note that here we distribute the space and time parts of $(2\pi)^4$ differently: the space part, $(2\pi)^3$, becomes $1/V$, because we replace $\int d^3\mathbf{q}$ by $\sum_{\mathbf{G}} \sum_{\mathbf{q}}$.

Since there are n free momentum variables and n Coulomb interaction lines, we can attribute the $1/V$ factor to the interaction line, and we can also attribute it to the sum over \mathbf{q} . In [7], the $1/V$ factor comes together with $v(\mathbf{q} + \mathbf{G})$. Indeed, they define

$$v(\mathbf{q} + \mathbf{G}) = \frac{4\pi e^2}{V|\mathbf{q} + \mathbf{G}|^2}. \quad (1.29)$$

The time part, 2π , now comes with integrations of ω 's. Thus, a ring diagram should be interpreted as



$$= \int \frac{d\omega}{2\pi} \sum_{m,n} iG_n^0(\mathbf{k}, \omega) iG_m^0(\mathbf{q} - \mathbf{k}, \omega_0 - \omega), \quad (1.30)$$

where $q = (\omega_0, \mathbf{q})$.

Another way to make sense of the Feynman rules in this section is to write down the Coulomb interaction Hamiltonian in the crystal momentum representation before deriving Feynman rules. The interaction Hamiltonian – the Coulomb repulsion Hamiltonian – is

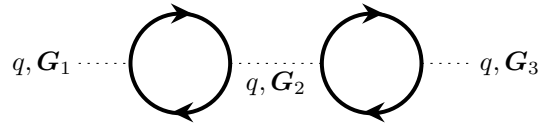
$$H = \sum_{1,2,3,4} c_4^\dagger c_3^\dagger H_{4321} c_2 c_1, \quad (1.31)$$

$$H_{4321} = \frac{1}{2} \int d^3\mathbf{r} \int d^3\mathbf{r}' \langle 4 | \mathbf{r} \rangle \langle 3 | \mathbf{r}' \rangle \langle \mathbf{r}' | 2 \rangle \langle \mathbf{r} | 1 \rangle v(\mathbf{r} - \mathbf{r}'), \quad (1.32)$$

Now again invoking the Fourier transformation from $v(\mathbf{r} - \mathbf{r}')$ to $v(\mathbf{q})$, and discretize the integration over \mathbf{q} , the $1/V$ factor appears again. The $1/2$ prefactor is canceled in the same way it's canceled in the free-space case.

1.1.2.3 Diagrammatic components as tensors

Both the Coulomb interaction line and the band electron propagator line contains one discrete index. And there are actually *two* indices: for an interaction-corrected Coulomb line, the two edges of a W line can have different \mathbf{G} vectors, as is clearly shown below:



For the renormalized electron Green function, the same applies.

Note that for a free-space electron, the band index label n is essentially \mathbf{G}_n , but once the crystal potential and the self-energy is added, electrons can be scattered from one \mathbf{G} to another. One may want to diagonalize the effective Hamiltonian, but now the band index after diagonalization no longer corresponds to the index of \mathbf{G} vectors.

Thus, the \mathbf{G} - and n -summations mentioned in Section 1.1.2.2 can be recast into matrix forms:

$$\longrightarrow^k = iG_{\mathbf{k}}^0(\omega) := i[\delta_{nn'}G_{n\mathbf{k}}^0(\omega)]_{nn'}, \quad (1.33)$$

$$\cdots^q = -iv(q) := -i[\delta_{\mathbf{G}\mathbf{G}'}v(\mathbf{q} + \mathbf{G})]_{\mathbf{G}\mathbf{G}'}, \quad (1.34)$$

and

$$\begin{array}{c} k \\ \swarrow \\ \text{---}^q \text{---} \\ \searrow \\ k+q \end{array} = M := [\langle n, \mathbf{k} + \mathbf{q} | e^{i(\mathbf{q} + \mathbf{G}) \cdot \mathbf{r}} | n' \mathbf{k} \rangle]_{nn' \mathbf{G}}, \quad (1.35)$$

$$\begin{array}{c} k \\ \swarrow \\ \text{---}^q \text{---} \\ \searrow \\ k+q \end{array} = M^* = [\langle n' \mathbf{k} | e^{-i(\mathbf{q} + \mathbf{G}) \cdot \mathbf{r}} | n, \mathbf{k} + \mathbf{q} \rangle]_{nn' \mathbf{G}}. \quad (1.36)$$

How to contract the indices can be done by following the standard quantum mechanic convention: the index of what happens later appears on the left side.

1.1.3 Quasiparticles

In the context of *ab initio* calculations, the term quasiparticle usually means renormalized band electrons and holes. Bosonic modes are just called “excitations”, and non-electron-like fermionic modes like spinons are simply absent (we are studying weakly correlated systems, anyway), so this terminology creates no confusion.

1.1.4 Light-matter interaction

1.1.4.1 Interaction Hamiltonian

The non-relativistic minimal coupling is

$$H = \frac{(\mathbf{p} - q\mathbf{A})^2}{2m} = \frac{(\mathbf{p} + e\mathbf{A})^2}{2m}, \quad (1.37)$$

and therefore the full light-matter interaction Hamiltonian is

$$H_{\text{light-matter}} = \frac{e\mathbf{p} \cdot \mathbf{A}}{m} + \frac{e^2 \mathbf{A}^2}{2m}. \quad (1.38)$$

Usually, the double-photon process is ignored, and we get

$$H_{\text{light-matter}} = \frac{e\mathbf{p} \cdot \mathbf{A}}{m}. \quad (1.39)$$

Note that here \mathbf{p} is the original momentum operator, i.e. $-i\nabla$.

The dipole approximation is

$$H_{\text{light-matter}} = -\mathbf{d} \cdot \mathbf{E}. \quad (1.40)$$

It can be derived when the effect of the outside electromagnetic field is predominantly electrostatic, and the system in question is restricted to a relatively small region. With the above two approximations, we can attribute the light-matter interaction to

$$H_{\text{light-matter}} = q\varphi \approx \text{const} + q\mathbf{r} \cdot \nabla\varphi \simeq \underbrace{q\mathbf{r}}_{-\mathbf{d}} \cdot \mathbf{E}. \quad (1.41)$$

Of course, when magnetic response of the system is important, we also need to add a magnetic dipole interaction term, etc.

Another light-matter interaction Hamiltonian is

$$H_{\text{light-matter}} = e\mathbf{v} \cdot \mathbf{A}. \quad (1.42)$$

The problem with this Hamiltonian is, when the potential term is not $V(\mathbf{r})$, we have

$$\mathbf{v} = \frac{1}{i}[\mathbf{r}, H] = \frac{\mathbf{p}}{m} + \frac{1}{i}[\mathbf{r}, \underbrace{V}_{\neq 0}]. \quad (1.43)$$

TODO: then why it works?

1.1.4.2 How to capture absorption

Absorption is usually modeled by the imaginary part of ϵ , and it's usually calculated by Fermi golden rule. There seems to be a contradiction here: Fermi golden rule looks “discrete”, while $\text{Im} \epsilon$ gives us a continuous damping.

Recall how we treat spontaneous radiation using a quantum jump formalism: damping here is introduced by two (related) factors, the first being $\text{Im} H_{\text{eff}}$, the second being the quantum jump channels, and once the shapes of the two terms in the master equation are determined, the strengths of which are “equal” to some extent.

Now $\text{Im} \epsilon$ is about $\text{Im} H_{\text{eff}}$, while Fermi golden rule is about the quantum jump channels, so it's indeed correct to infer $\text{Im} \epsilon$ from Fermi golden rule, using a procedure like, say, comparing the amount of light absorbed calculated from $\text{Im} \epsilon$ and from Fermi golden rule. There is no double counting in this procedure: *both* $\text{Im} H_{\text{eff}}$ and Γ are needed for a full account of dissipation. H_{eff} continuously reduces the possibility to see the system staying in its original state, while quantum jump channels “confirm” that indeed the system decays to a lower energy state when the norm of the wave function has decreased considerably.

In the phenomenological model of spontaneous radiation, we first write down an H_{eff} , and then find the correct corresponding quantum jump channels to make the theory unitary, while here, we first calculate quantum jump channels (i.e. scattering) and then fit the H_{eff} according to the strength of scattering.

1.2 Overview of $GW+BSE$

1.2.1 What is GW

1.2.1.1 GW is screened Hartree-Fock approximation

In short, GW means

$$\Sigma = iGW, \quad (1.44)$$

where G is the renormalized Green function, and W is the renormalized (i.e. screened) Coulomb interaction, which is

$$W = \frac{v}{\epsilon} = \dots + \dots \bigcirc \dots + \dots \bigcirc \dots \bigcirc \dots + \dots, \quad (1.45)$$

$$\epsilon = 1 - \dots \bigcirc \dots. \quad (1.46)$$

Compared with the exact Hedin equations, no vertex correction is taken into account here in GW .

It should be noted that the ϵ here is a matrix, but it contains no index of the ordinary 3-vector: it's a *scalar* in the real space, because it connects W and v , both of which are scalar potentials. The *dielectric matrix* used to connect vector \mathbf{E} and \mathbf{D} is related to $\epsilon_{\mathbf{G}\mathbf{G}'}$ (TODO: how?) but they are not simply equal.

1.2.1.2 GW compared with the Hartree-Fock approximation

Note that there *is* screening in self-consistent Hartree-Fock approximation: if we forget about the Fock term, then the Hartree approximation is essentially the same as Thomas-Fermi screening, which considers and only considers screening channels with respect to *density of electrons*, i.e. ring diagrams. Then we add the Fock term, and in the Fock term, there is still screening in the corrected propagator, but there is no screening in the Coulomb interaction line. (On the other hand, in the Hartree term, there shouldn't be any screening in the Coulomb interaction line, or otherwise we have double counting.)

In this perspective, GW is completely natural: the next level of correction is just to correct the Coulomb interaction line, using the same ring diagrams that appear in the self-consistent Hartree term.

1.2.1.3 BSE with the same order of approximation

TODO:

- Truncated Coulomb interaction
- Derive

$$\text{Im } \epsilon = \frac{16\pi^2 e^2}{\omega^2} \sum_S |\hat{e} \cdot \langle 0 | \mathbf{v} | S \rangle|^2 \delta(\omega - \Omega^S). \quad (1.47)$$

- Why we say $\Sigma = V_{xc} + \Sigma - V_{xc}$? (see [5] p. 1271)
- What should be symmetric? (11) and (12) in [5]???

1.2.2 The ϵ matrix

1.2.2.1 Frequency-dependent form

To build concrete expressions from the above floppy arguments, let's apply the rules in Section 1.1.2.3. First, we define

$$q \cdots \cdots \text{---} \bigcirc \text{---} \cdots \cdots q = i\chi(q) \quad (1.48)$$

Here the dotted lines are dummies: they contribute nothing to the value of the diagram. Note that χ is a matrix, with its elements taking the form of $\chi_{\mathbf{G}\mathbf{G}'}$.

Now we have (every letter in the expression below is a matrix, so pay attention to the order)

$$-iW(q) = -iv(q) + (-iv(q))(i\chi(q))(-iv(q)) + \cdots,$$

$$W(q) = v(q) + v(q)\chi(q)v(q) + v(q)\chi(q)v(q)\chi(q)v(q) + \cdots = (1 - v(q)\chi(q))^{-1}v(q).$$

So we get a concrete expression of ϵ :

$$\epsilon(q) = 1 - v(q)\chi(q), \quad W(q) = \epsilon(q)^{-1}v(q). \quad (1.49)$$

Because

$$(v(q)\chi(q))_{\mathbf{G}\mathbf{G}'} = \sum_{\mathbf{G}''} v(q + \mathbf{G}'') \delta_{\mathbf{G}\mathbf{G}''} \chi_{\mathbf{G}''\mathbf{G}'}(q).$$

we have

$$\epsilon_{\mathbf{G}\mathbf{G}'}(q) = \delta_{\mathbf{G}\mathbf{G}'} - v(q + \mathbf{G})\chi_{\mathbf{G}\mathbf{G}'}(q). \quad (1.50)$$

Here the inverse of ϵ is matrix inverse, not element-by-element inverse. (13) in [5] is ambiguous: a clearer but more cumbersome notation is

$$[\epsilon_{\mathbf{G}\mathbf{G}'}(q)]_{\mathbf{G}\mathbf{G}'}^{-1} v(q + \mathbf{G}').$$

Now it comes the evaluation of $\chi_{GG}(q)$. Under the quasiparticle assumption, that the renormalized Green function can still be written as (1.19), We have

$$\begin{aligned}
i\chi_{GG'}(\mathbf{q}, \omega) &= q, G \overset{n, k+q}{\curvearrowright} q, G' \\
&\quad n', k \\
&= - \int \frac{d\omega'}{2\pi} \sum_{\mathbf{k}} \sum_{n, n'} \frac{i}{\omega' - \xi_{n'\mathbf{k}} + i0^+ \text{sgn}(\xi_{n'\mathbf{k}})} \frac{i}{\omega + \omega' - \xi_{n, \mathbf{k}+\mathbf{q}} + i0^+ \text{sgn}(\xi_{n, \mathbf{k}+\mathbf{q}})} \\
&\quad \times M_{nn'}(\mathbf{k}, \mathbf{q}, \mathbf{G}) M_{nn'}^*(\mathbf{k}, \mathbf{q}, \mathbf{G}'),
\end{aligned} \tag{1.51}$$

where the minus sign comes from the closed electron loop, and to make the final expression agree with [5], I choose a rather strange direction of the \mathbf{q} arrow. The bands and wave functions are all renormalized ones.

The RHS of the equation can be evaluated straightforwardly: when $\xi_{n',\mathbf{k}} < 0$, $\xi_{n,\mathbf{k}+\mathbf{q}} > 0$, we have

$$\begin{aligned} & \int \frac{d\omega'}{2\pi} \frac{1}{\omega' - \xi_{n'\mathbf{k}} + i0^+ \operatorname{sgn}(\xi_{n'\mathbf{k}})} \frac{1}{\omega + \omega' - \xi_{n,\mathbf{k}+\mathbf{q}} + i0^+ \operatorname{sgn}(\xi_{n,\mathbf{k}+\mathbf{q}})} \\ &= \int \frac{d\omega'}{2\pi} \frac{1}{\omega' - \xi_{n'\mathbf{k}} - i0^+} \frac{1}{\omega + \omega' - \xi_{n,\mathbf{k}+\mathbf{q}} + i0^+} \\ &= \frac{2\pi i}{2\pi} \frac{1}{\omega + \xi_{n'\mathbf{k}} + i0^+ - \xi_{n,\mathbf{k}+\mathbf{q}} + i0^+}, \end{aligned}$$

where in the third line we complete the integral contour in the upper plane. Similarly, when $\xi_{n'\mathbf{k}} > 0$, $\xi_{n,\mathbf{k}+\mathbf{q}} < 0$, we have

$$\begin{aligned}
& \int \frac{d\omega'}{2\pi} \frac{1}{\omega' - \xi_{n'\mathbf{k}} + i0^+ \operatorname{sgn}(\xi_{n'\mathbf{k}})} \frac{1}{\omega + \omega' - \xi_{n,\mathbf{k}+\mathbf{q}} + i0^+ \operatorname{sgn}(\xi_{n,\mathbf{k}+\mathbf{q}})} \\
&= \int \frac{d\omega'}{2\pi} \frac{1}{\omega' - \xi_{n'\mathbf{k}} + i0^+} \frac{1}{\omega + \omega' - \xi_{n,\mathbf{k}+\mathbf{q}} - i0^+} \\
&= \frac{2\pi i}{2\pi} \frac{1}{-\omega + \xi_{n,\mathbf{k}+\mathbf{q}} + i0^+ - \xi_{n'\mathbf{k}} + i0^+}
\end{aligned}$$

When $\xi_{n'\mathbf{k}}$ and $\xi_{n,\mathbf{k}+\mathbf{q}}$ are both positive or negative, the integral is zero. Thus, we find

$$\chi_{GG'}(\mathbf{q}, \omega) = \sum_{\mathbf{k}} \sum_{n, n'} M_{nn'}(\mathbf{k}, \mathbf{q}, \mathbf{G}) M_{nn'}^*(\mathbf{k}, \mathbf{q}, \mathbf{G}') \times \left(\frac{\theta(-\xi_{n'\mathbf{k}}) \theta(\xi_{n, \mathbf{k}+\mathbf{q}})}{\omega + \xi_{n'\mathbf{k}} - \xi_{n, \mathbf{k}+\mathbf{q}} + i0^+} + \frac{\theta(\xi_{n'\mathbf{k}}) \theta(-\xi_{n, \mathbf{k}+\mathbf{q}})}{-\omega + \xi_{n, \mathbf{k}+\mathbf{q}} - \xi_{n'\mathbf{k}} + i0^+} \right). \quad (1.52)$$

TODO: occupied, or empty:

Note that in [5], the normalization of χ is the same as here, but the definition of $v(\mathbf{q})$ doesn't include the $1/V$ factor. So (8) in [5] is wrong: it leads to a ridiculous result: as we increase the density of the \mathbf{k} -grid, χ becomes larger and larger!

1.2.2.2 The static limit and the generalized plasmon-pole model

In the $\omega \rightarrow 0$ limit, we have

$$\chi_{GG'}(\mathbf{q}, \omega = 0) = \sum_{\mathbf{k}} \sum_{n, n'} M_{nn'}(\mathbf{k}, \mathbf{q}, \mathbf{G}) M_{nn'}^*(\mathbf{k}, \mathbf{q}, \mathbf{G}') \times \left(\frac{\theta(-\xi_{n'\mathbf{k}}) \theta(\xi_{n, \mathbf{k}+\mathbf{q}})}{\varepsilon_{n'\mathbf{k}} - \varepsilon_{n, \mathbf{k}+\mathbf{q}}} + \frac{\theta(\xi_{n'\mathbf{k}}) \theta(-\xi_{n, \mathbf{k}+\mathbf{q}})}{\varepsilon_{n, \mathbf{k}+\mathbf{q}} - \varepsilon_{n'\mathbf{k}}} \right). \quad (1.53)$$

1.3 Accuracy of GW

1.3.1 Coverage

GW proves to be accurate enough for most weakly-correlated systems. TODO: any counter-examples? Recently, it's also applied successfully to systems like polymers, nano-wires and molecules.

1.3.2 Diagonal or not

We know in the momentum space, we have

$$E_{n\mathbf{k}}^{\text{QP}} = E_{n\mathbf{k}}^0 + \Sigma_{n\mathbf{k}}(E^{\text{QP}}). \quad (1.54)$$

Here since Σ depends on the corrected propagator, $E_{n\mathbf{k}}^{\text{QP}}$ enters its expression. The cost of GW calculation means we need to first do a DFT calculation and feed this as the input of the GW package (the former usually mysteriously called the “mean field” step, though we may also say GW is a mean-field method; on the other hand, in principle – though of course not in practice – DFT is able to decide everything about the system), so (1.54) now is

$$E_{\mathbf{k}}^{\text{QP}} = E_{\mathbf{k}}^{\text{KS}} + \Sigma_{\mathbf{k}}(E^{\text{QP}}) - \Sigma^{\text{KS}}. \quad (1.55)$$

Here Σ^{KS} is the so-called DFT self-energy, i.e. the Hartree potential plus the exchange-correlation potential. Note that here I don't insert band indices into the equation, because $\Sigma_{\mathbf{k}}$ may mix different bands together, and (1.55) is an equation about matrices, essentially a single-electron Schrodinger equation. It's first order approximation is

$$E_{n\mathbf{k}}^{\text{QP}} = E_{n\mathbf{k}}^{\text{KS}} + \langle \psi_{n\mathbf{k}}^{\text{KS}} | \Sigma(E_{n\mathbf{k}}^{\text{QP}}) - \Sigma^{\text{KS}} | \psi_{n\mathbf{k}}^{\text{KS}} \rangle. \quad (1.56)$$

TODO: when doing iterative calculation, V_{H} may no longer be the same between DFT and GW ?? So when doing iterative calculation, should we calculate “the GW V_{H} ”?

1.3.3 Self-consistent or not

There are three iterative schemes. The first is the eigenvalue self-consistent scheme: It's just a self-consistent solver of (1.56). In this case, we don't need off-diagonal elements, because they are not used in (1.56). This scheme is mentioned in Section 3.3 in [5]. The second scheme takes the change of eigenvalues into account, and thus iteratively solves (1.55). In this case we need to take non-diagonal elements seriously [1,6]. In the third scheme, the form of Σ itself is changed: Recall that we need an `epsilon` step to calculate ϵ and thus the screened interaction potential W , and $\Sigma = iGW$. This in general is not recommended, because we know GW tends to widen the band gap, and sometimes as we iteratively update the band gap, it becomes too large. The origin of this overestimation of band gap is that GW neglects the vertex, so iterative GW only leads us towards the more and more inaccurate way.

The non-self-consistent G_0W_0 calculation proves to be a better choice empirically, if the initial DFT input is of good quality – and here there is another empirical observation that sometimes LDA functional together with G_0W_0 provides better results. Still, the argumentation provided above only explains why iterative GW is bad, but doesn't explain why one-shot GW is good. In other words, we need to know how certain factors in the one-shot GW scheme somehow makes up for the missing vertex correction.

One possible form of the vertex is the electron-hole interaction, which is calculated by solving the BSE. Now an empirical fact is LDA tends to give the same band gap as BSE, leading to a pretty good one-shot approximation.

TODO: [11]

The question, then, is why LDA in some cases works as well as BSE. The reason for this is because of the relation between the derivative discontinuity in DFT and electron-hole interaction kernel TODO: the relation with [9]

1.3.4 On so-called failure of GW and convergence issues

Some (weak-correlated, of course) materials are claimed to be impossible to be characterized correctly using GW , or at least G^0W^0 . [10] refutes such a claim, at least for ZnO.

The root for this seems to be poor convergence test: people often use insufficient number of bands, etc.

See <https://www.nerisc.gov/assets/Uploads/ConvergenceinBGW.pdf>

1.4 The QuantumESPRESSO-BerkeleyGW ecosystem

1.4.1 Overview of the pipeline

TODO: whether and how BerkeleyGW supports HSE06. See <https://groups.google.com/a/berkeleygw.org/g/help/c/I>

Note that the division of labor is different in the GW step and the BSE step. The **sigma** program doesn't really do diagonalization, so building Σ and finding quasiparticle energies are done in one step, which is implemented in **sigma**. On the other hand, diagonalization *is* needed for BSE, so building the kernel – counterpart of Σ – is done in one step (**kernel**), while diagonalizing it is done in another step (**absorption**).

1.4.2 Relativistic effects

BerkeleyGW supports SOC calculation, with the so-called fully relativistic mode and the scalar relativistic mode; I say “so-called” because all the calculations are still done in the framework of Schrodinger equation, with relativistic effects being introduced by adding perturbative terms like $\mathbf{L} \cdot \mathbf{S}$ or \mathbf{p}^4 [2]. On the other hand, when it comes to calculating the inner structure of atoms (which, in condensed matter physics, is usually seen when we generate our own pseudopotentials), being “fully relativistic” means using *Dirac equation*.

1.4.3 Input and output of pw

1.4.4 epsilon

1.4.4.1 Procedure and speed

What **epsilon** does, as its name implies, is to calculate ϵ – and since ϵ is used to find W , we need ϵ^{-1} . The relative equations are (8-10) in [5]. There are three steps in **epsilon**:

1. Calculate $M_{nn'}(\mathbf{k}, \mathbf{q}, \mathbf{G})$;
2. Summing over n, n', \mathbf{k} ;
3. Finding ϵ^{-1} .

With a fixed accuracy requirement, the time cost of first step is $\sim N^3 \log N$, where N is the number of atoms per unit cell. The \mathbf{k} and \mathbf{q} points are given by the \mathbf{q} -grid given in **epsilon.inp** and the \mathbf{k} -grid in the wave function files, so they are fixed are not a part of the scaling. With the cutoff energy fixed, the size of the \mathbf{G} -grid is proportional to V , which is in turn proportional to N (the distance between atoms is roughly fixed, and therefore the more atoms we have, the larger the unit cell is). With a fixed accuracy standard, the required numbers of occupied bands and empty bands are all $\sim N$, so the number of matrix elements of $M_{nn'}(\mathbf{k}, \mathbf{q}, \mathbf{G})$ scales as N^3 . For each matrix element, we need to calculate $\langle n, \mathbf{k} + \mathbf{q} | e^{i(\mathbf{q} + \mathbf{G}) \cdot \mathbf{r}} | n', \mathbf{k} \rangle$. Note that the matrix inside contains only \mathbf{r} , and the expression therefore can be evaluated as

$$\int d^3\mathbf{r} \phi_{n, \mathbf{k} + \mathbf{q}}^*(\mathbf{r}) e^{i(\mathbf{q} + \mathbf{G}) \cdot \mathbf{r}} \phi_{n', \mathbf{k}}(\mathbf{r}),$$

and the scale of the calculation needed is proportional to V and again N . In practice, we use the \mathbf{G} representation to calculate the matrix element, and again the time cost is $\sim N$. (Note that the two estimations are equivalent: by saying the time cost is proportional to V , we implicitly imply the absolute spatial resolution is fixed, which, in other words, means we fix the cutoff energy.) So naively, the time cost is $\sim N^4$. Fortunately the matrix element $M_{nn'}(\mathbf{k}, \mathbf{q}, \mathbf{G})$ with

fixed n, n', \mathbf{G} can be evaluated by fast Fourier transformation, so eventually, the time cost scales like $N^3 \log N$.

The time cost of the second step, in a serial program, scales like N^4 . We sum over n and n' , each of which has $\sim N$ values. And we need to calculate $\chi_{\mathbf{G}\mathbf{G}'}$, where the values of \mathbf{G} and \mathbf{G}' are all roughly proportional to N . So the final scaling of the time cost is N^4 . This however can be parallelized, and eventually, in a well optimized parallelized package, the time cost scales like N^2 .

The time cost of the third step – the matrix inversion step – scales like N^3 .

1.4.4.2 Divergence problems when $\mathbf{q} \rightarrow 0$

When calculating $\epsilon_{\mathbf{G}\mathbf{G}'}(\mathbf{q}, \omega = 0)$, we notice that when $\mathbf{G} = \mathbf{G}' = 0$, the matrix element diverges as $\mathbf{q} \rightarrow 0$. For an insulator, we have

$$\begin{aligned} \epsilon_{00}(\mathbf{q} \rightarrow 0, \omega = 0) &\propto -\frac{1}{q^2} \chi_{00}(\mathbf{q} \rightarrow 0, \omega = 0) \\ &\propto \sum_{n \text{ occupied}, n' \text{ empty}} -\frac{1}{q^2} |\langle n\mathbf{k} | 1 + i(\mathbf{q} + \mathbf{G}) \cdot \mathbf{r} + \dots | n'\mathbf{k} \rangle|^2 \\ &\propto \text{const.} \times \frac{q^2}{q^2}. \end{aligned} \quad (1.57)$$

Here the first term in the Taylor expansion of $e^{i(\mathbf{q}+\mathbf{G})\cdot\mathbf{r}}$ vanishes because of orthogonality conditions. We see $\epsilon_{00}(\mathbf{q} \rightarrow 0, \omega = 0)$ has a definite value.

For a metal, some bands are both occupied and empty, so we can no longer use the orthogonality conditions, and $\epsilon_{00}(\mathbf{q} \rightarrow 0, \omega = 0)$ scales like C/q^2 . TODO: whether this is a numerical artifact or not To decide the constant C , very fine description of the Fermi surface is needed, so we need a very fine \mathbf{k} -grid. On the other hand, we don't really need many bands, because for the metal $\epsilon_{00}(\mathbf{q} \rightarrow 0, \omega = 0)$, most of the relevant transitions are inter-band ones.

1.4.4.3 Frequency dependence of ϵ

The $\epsilon_{\mathbf{G}\mathbf{G}'}(\mathbf{q}, \omega)$ matrix has frequency dependence. The fastest way to handle this is to calculate the $\omega = 0$ case only and then find the plasmon frequency, and then, the $\epsilon_{\mathbf{G}\mathbf{G}'}(\mathbf{q}, \omega)$ curve can be fitted using sum rules. TODO

The spectral function – used in ARPES simulation – can't be accurately obtained just by the above mentioned method. Thus, **full frequency** treatments are needed. A trick called **static subspace** can speed up the process. TODO

1.4.4.4 Console output

The console output of `epsilon` has the following structure:

1. Initialization
2. Iterating over the \mathbf{q} -grid. For each \mathbf{q} -point,
 - (a) The output starts with something like

```
=====
13:59:21   Dealing with q =  0.000000  0.500000  0.000000      5 / 35
=====
```

```
This is a regular non-zero q-point.
```

- (b) Then we can see lines about Rank of the polarizability matrix, BLACS processor grid, and Number of k-points in the irreducible BZ(q) (nrk).
- (c) Now we enter the first step mentioned in Section 1.4.4.1. The start line looks like

```
Started calculation of matrix elements with 324 transition(s) at
↪ 13:59:21.
```

- (d) TODO: what's the corresponding step of the following line:

```
Started building polarizability matrix with 320 processor(s) at
↪ 13:59:30.
```

1.4.4.5 Other output files

The `epsilon` program generates the files mentioned in [this page](#). Note that `eps0mat.h5` is *not* ϵ from DFT orbitals! In steps after `epsilon`, screening obtained from DFT orbitals are not used; we only use ϵ from *GW* orbitals. The file `eps0mat.h5` is the ϵ around the Γ point. Thus, in principle, we can calculate `eps0mat.h5` and `epsmat.h5` in two runs, and indeed this is the case when we deal with a metallic system (Section [3.1.4](#)).

1.4.5 Systems of units

TODO

Chapter 2

Tight-binding models

TODO: from ab initio to models

2.1 Wannier functions and tight-binding models

For an insulator, we can construct exponentially decaying Wannier functions if and only if the Chern numbers are zero, and thus all insulators with inversion symmetry have exponentially decaying Wannier functions [3]

[8] introduces Maximally localized Wannier functions.

Chapter 3

Carrying out calculations

3.1 Standard operation procedures

3.1.1 Avoid data pollution

The follows are strongly recommended whenever modifying files:

- Read out loud the *directory* of the file being modified. Are you mistakenly modify files in another directory?
- When copying file from a folder to another, similarly read out loud the name of the source and the target.
- If a file is going to be overwritten, make sure it's really no longer needed. Whenever you have doubts, make backups.
-

3.1.2 Structural relaxation

TODO: Wyckoff positions

3.1.3 Insulator DFT+ GW +BSE

3.1.3.1 The DFT stage

1. Do a `scf` calculation in `1-scf`.
2. Do a `bands` calculation in `2.1-wfn`. This step includes:
 - (a) Create a `the-suffix-you-set.save` folder in `2.1-wfn`, and link `data-file-schema.xml` and `charge-density.dat` from `1-scf` into this folder. These are files required for a `bands` calculation.
 - (b) Run

```
data-file2kgrid.py --kgrid nx ny nz the-suffix-you-set.save/  
→ data-file-schema.xml kgrid.inp
```

to create `kgrid.inp`, which describes how to create a k -grid with size `nx ny nz`. This can't be done with options in QuantumESPRESSO's `KPOINTS` section because QuantumESPRESSO and BerkeleyGW have different tolerance for symmetry.

- (c) Run

```
kgrid.x kgrid.inp kgrid.out kgrid.log
```

to obtain `kgrid.out`. The content in `kgrid.out` will be used as the `KPOINTS` section for the input file of `pw`.

- (d) Preparing the `bands.in` file, which is the input file of `pw.x`. Do the following checklist:
 - Whether calculation is `bands`.
 - Whether `pseudo_dir` is correct.

- Whether `nbnd` is set to, say, 1000.
 - Whether `lspinorb = .true.` and `noncolin = .true.` are set for an SOC run.
- (e) Run `pw2bgw.x` in 2.1-wfn. Do the following checklist:
- This step should be done with *exactly the same* parallelization setting with `pw.x`.
 - The `wfng_nk1`, `wfng_nk2`, `wfng_nk3` parameters should be set to `nx`, `ny`, `nz` mentioned above. (This item needs double check especially when `pw2bgw.inp` comes from another run.)
 - Whether `rhog_flag` is `.true..`
 - Whether `vxc_flag` is `.true..`
 - Whether `wfng_flag` is `.true..`
3. Do a `bands` calculation in 2.2-wfnq. The steps are similar to 2.1-wfn:
- (a) Linking files from 1-scf.
- (b) Run

```
data-file2kgrid.py --kgrid nx ny nz --qshift qx qy qz the-
→ suffix-you-set.save/data-file-schema.xml kgrid.inp
```

to get the `kgrid.inp` file. Here `qx qy qz` is a small displacement used to regularize Coulomb interaction at $\mathbf{q} = 0$. A common choice is 0 0 0.001; when dealing with a 2D material, choose 0 0.001 0, because with `cell_slab_truncation` open in the `epsilon.x` step, non-zero z components of \mathbf{k} -points are forbidden.

- (c) Run `kgrid.x`.
- (d) Preparing the `bands.in` file.
- (e) Run `pw2bgw.x`. Do the following checklist:

- This step should be done with *exactly the same* parallelization setting with `pw.x`.
- The `wfng_nk1`, `wfng_nk2`, `wfng_nk3` parameters should be set to `nx`, `ny`, `nz` mentioned above.
- The `wfng_dk1`, `wfng_dk2`, `wfng_dk3` parameters should be set to `wfng_nk1 × qx`, etc. (If `kshift` is used, it also should be added to `wfng_dk1`, etc.)

Note that this doesn't mean the displacement imposed to the \mathbf{k} -grid is `wfng_nk1 × qx`: the displacement is still `qx qy qz`. Here the `wfng_dk1`, `wfng_dk2`, `wfng_dk3` are conventional parameters used in Monkhorst-Pack grids, and `wfng_dk1 = 0.5` means the grid is shifted towards x direction by half a *grid step* – and therefore the displacement is $0.5 \times 1 / \text{wfng_nk1}$ in the crystal coordinates. Now we understand why we need to set `wfng_dk1` to `wfng_nk1 × qx`. Indeed, below is a part of the header of a WFN file in 2.2-wfnq:

```
k-grid:    24  24    1
k-shifts:    0.000000    0.024000    0.000000
[ifmin = lowest occupied band, ifmax = highest occupied band, for
→ each spin]
  Index      Coordinates (crystal)      Weight    Number of
  → G-vectors    ifmin    ifmax
    1    0.000000    0.001000    0.000000    0.001736
  →                      36275          1    120
```

It can be seen that the first \mathbf{k} -point is displaced 0.001 in the y direction, and the `k-shifts` parameter corresponding to the y direction is 0.024; since the size of the grid in the y direction is 24, the displacement instructed by the latter is $0.024/24 = 0.001$, exactly the displacement recorded in the first \mathbf{k} -point.

3.1.3.2 The GW stage

1. Do a `epsilon` calculation in 1-epsilon. The steps are listed below:
- (a) Linking files. Come to 1-epsilon and do the follows:

```
ln -sf ../2.1-wfn/WFN
ln -sf ../2.2-wfnq/WFN ./WFNq
```

- (b) Prepare `epsilon.inp`. Do the follow checklist:
- Whether we are setting `qpoints` instead of `kpoints`.

- Whether there is an `end` line of the `qpoints` block.
- Whether each line of the `qpoints` block is in the format (see [here](#))

```
qx qy qz 1 is_q0
```

- Especially, whether the line corresponding to the Γ point has `is-q0 = 1`.
- If we are dealing with a 2D material, add `cell_slab_truncation`.
- Set `epsilon_cutoff` to, say, 10; the exact value is to be decided by convergence tests.
- Set `number_bands` to the highest *total* number of bands allowed by `degeneracy_check.x` (Section [4.3.1](#)).

2. Do a `sigma` calculation in `2-sigma`. The steps are listed below:

(a) Link necessary files:

```
ln -sf ../2.1-wfn/vxc.dat
ln -sf ../2.1-wfn/RH0
ln -sf ../2.1-wfn/WFN ./WFN_inner
ln -sf ../1-epsilon/epsmat.h5
ln -sf ../1-epsilon/eps0mat.h5
```

(b) Prepare `sigma.inp`. Do the following checklist:

- Whether we are setting `kpoints` instead of `qpoints`. (This time it's not `qpoints`!)
- Whether there is an `end` line of the `kpoints` block.
- Whether each line of the `kpoints` block is in the format

```
kx ky kz 1
```

- If we are dealing with a 2D material, add `cell_slab_truncation`.
- Set `number_bands` to the same value in `epsilon.inp`.
- Set `band_index_min` and `band_index_max`. The bands between the two are corrected by ([1.54](#)), and others are not.

3.1.3.3 The BSE stage

1. Do a `kernel` calculation in `3-bse`. The steps are listed below:

(a) Link necessary files.

```
ln -sf ../1-epsilon/WFN ./WFN_co
ln -sf ../1-epsilon/epsmat.h5
ln -sf ../1-epsilon/eps0mat.h5
```

(b) Prepare `kernel.inp`. Do the following checklist:

- Whether the following lines are there:

```
use_symmetries_coarse_grid
```

- Whether `number_val_bands` and `number_cond_bands` are specified.
- If we are dealing with a 2D material, whether `cell_slab_truncation` is added.

2. Do an `absorption` step.

(a) Build a denser `k`-grid and repeat `2.1-wfn` and `2.2-wfnq` steps.

(b) Link necessary files.

```
ln -sf ../2.1-wfn/WFN ./WFN_co
ln -sf ../2.2-wfnq/WFN ./WFNq_co
ln -sf ../2.1-wfn-dense/WFN ./WFN_fi
ln -sf ../2.2-wfnq-dense/WFN ./WFNq_fi
ln -sf ../1-epsilon/epsmat.h5 ./
ln -sf ../1-epsilon/eps0mat.h5 ./
ln -sf ../3-kernel/bsema.h5 ./
```

The `bsema` and `msexmat` files are missing if HDF5 format is used to generate the output files – the documentation of BerkeleyGW says we need the files but it's wrong: When `bsema.h5` is present, the program runs well.

(c) Prepare `absorption.inp`. Do the following checklist:

- Whether the following lines are in `absorption.inp`:

```
use_symmetries_fine_grid
use_symmetries_coarse_grid
```

- Whether

```
number_cond_bands_coarse
number_cond_bands_fine
number_val_bands_coarse
number_val_bands_fine
```

are specified.

-

3.1.4 Metal DFT+GW+BSE

For metals, the q -displacement technique can no longer be used. The working procedure now is

1. Do a `scf` calculation in `1-scf`.
2. Do a `bands` calculation in `2.1-wfn`.
3. Do `2.2-wfn0` with a *finer* k -grid, still *without* any `qshift` displacement.
4. Do a `epsilon` calculation in `1-epsilon`. The steps are listed below:

- (a) Link files according to

```
ln -sf ../2.1-wfn/WFN
ln -sf ../2.1-wfn/WFN ../WFNq
```

The `2.2-wfnq` step is not needed, because we are not going to deal with the Γ point in this step.

- (b) Preparing `epsilon.inp`. Do the following checklist:

- Whether we are setting `eqpoints` instead of `kpoints`.
- Make sure the Γ point is *not* included in the `qpoints` block.
- Whether each line of the `qpoints` block is in the format

```
qx qy qz 1 0
```

5. Do a `epsilon` calculation in `1.2-epsilon0`.

- (a) Link files according to

```
ln -sf ../2.2-wfn0/WFN
ln -sf ../2.2-wfn0/WFN ../WFNq
```

Now the outputs of the `2.1-wfn` step is not used.

- (b) Prepare `epsilon.inp`. Do the following checklist:

- Whether we are setting `eqpoints` instead of `kpoints`.
- The *only point* included in the `qpoints` block should be the non-zero k -point with smallest length in the k -grid used in `2.2-wfn0`.
- Whether the Γ point is in the format

```
qx qy qz 1 2
```

3.1.5 Band plot

3.1.5.1 DFT level

The Fermi energy is to be found in `scf.out`. It won't appear in `bands.out`.

3.1.5.2 GW level: `inteqp`

The GW level bands can be obtained by the `inteqp` program. Note that this shouldn't be used for a system considered metallic by DFT (Section 4.6.4). The standard operation procedure is listed here:

1. Go to `4-path` – the folder responsible for the DFT level calculation – and perform a `pw2bgw` run needed to create a WFN file. Note that if we are not dealing with a k -grid, `wfng_nk1`, `wfng_nk2`, and `wfng_nk3` should be skipped.
2. Create a folder within `1-epsilon/`, and go into it.
3. Link the necessary files:

```
ln -sf ../../2.1-wfn/WFN ./WFN_co
ln -sf ../../4-path/WFN ./WFN_fi
cp ../../1-epsilon/eqp1.dat ./eqp_co.dat
```

4.

3.1.5.3 BSE level

3.1.6 Wannier functions and tight-binding models

Tight-binding models are a more compact way to show the band structure.

3.1.6.1 wannier90 for DFT

1. The first step is to perform a fresh QuantumESPRESSO run. `wannier90` requires a full Monkhorst–Pack grid, and to create a `bands.in` file, (don't forget to add the `utility` folder to the `PATH` environment variable) just prepare a `bands.in` file without the `K_POINTS` block and run

```
kmesh.pl 20 20 1 >> bands.in
```

Replace `20 20 1` by the k -grid size you want. The number of bands in this DFT run *shouldn't* be too large, or otherwise `pw2wannier90` will be extremely slow.

2. Prepare a `prefix.win` file, where `prefix` is the QuantumESPRESSO prefix used. Examples of this input file can be found by searching “wannier90 2007 workshop” and downloading the tutorial files coming together with the web page about this event – currently it's [here](#). Do the following checklist:
 - Is `num_bands` plus the number of excluded bands the same as `nbnd` in the QuantumESPRESSO run (Section 4.4.1)? If you don't want all valence bands in the DFT run, always decide how many bands to include *before* doing any `wannier90.x` run; changing parameters in `prefix.win` after a `wannier90.x` run may lead to inconsistencies.

3. Run

```
wannier90.x -pp prefix.win
```

to get `prefix.nnkp`.

4. Run `pw2wannier90.x`. The input file looks like

```
&inputpp
outdir      = './'
prefix      = 'WTe2'
seedname     = 'WTe2'
scdm_proj   = .true.
write_amn    = .true.
write_mmn    = .true.
write_unk    = .true.
/
```

This step should finish in several minutes. If it takes too long, reduce `nbnd` in the QuantumESPRESSO step and redo the whole procedure.

5. Run

```
wannier90.x prefix.win
```

3.1.6.2 *GW* level: sig2wan

The `sig2wan` code can extract a Wannier interpolated band structure from output files of the `sigma` step. An example can be found [here](#). The routine is almost the same as `wannier90` for DFT, except for one thing: after running `pw2wannier90.x`, we need to replace the `perfix.eig` file generated by `pw2wannier90.x` by the `prefix.eig` file generated by `sig2wan`.

3.1.7 Energy self-consistent calculation

The `epsilon` code has an option called `eqp_corrections`, which takes the

3.2 Performance tricks

3.2.1 Parallelization

TODO: Do more MPI tasks already result in faster speed?

3.2.2 Choosing cutoff energies wisely

The cutoff energies, especially the one in the *GW* step, of course should be large enough, but not too large: if in a benchmark test, a smaller cutoff energy gives almost the same result compared to a higher cutoff energy, then the smaller cutoff energy should be used unless we have reasons against this practice.

3.2.3 pseudobands

```
wfn2hdf.x BIN WFN WFN.h5
pseudobands.py WFN.h5 WFN.h5 0.7 0.02
hdf2wfn.x BIN WFN.h5 WFN
```

Using `pseudobands` breaks the norm conserving condition. Therefore, in `espilon.inp`, we need to add `dont_check_norms`.

TODO: how it works; maybe [\[4\]](#) may provide some hints.

3.3 Convergence tests

Chapter 4

Trouble shooting

4.1 Trouble shooting in MPI

4.1.1 error parsing parameters

This sometimes occurs because you misspell the name of a program to be `mpiruned`.

4.2 Trouble shooting in QuantumEspresso

4.2.1 Program frozen

Check whether too much resource is given to a simple task.

4.2.2 Error in routine `allocate_fft (1): wrong ngms`

I'm still not quite sure what causes this error, but it seems to be related to parallelization: in a run with 2240 MPI tasks, the error occurred, but when I used 320 MPI tasks, the error disappeared.

4.2.3 Error reading attribute `index : expected integer , found *`

This error occurs when we use a pseudopotential that is obtained by converting another pseudopotential in a different format (see [here](#)). Usually we don't need to "correct" it.

4.2.4 `cdiaghg (159): eigenvectors failed to converge`

Usually by changing `diagonalization` to `cg`, this can be solved; `cg` is more stable but much slower.

4.2.5 Error in routine `cdiaghg (1052): problems computing cholesky`

This also seems to be a convergence problem that can be solved by changing `diagonalization` to `cg`.

4.2.6 Error in routine `set_occupations (1): smearing requires a vaklue for gaussian broadening (degauss)`

This happens whenever smearing is used but the smearing parameter is not set. Note that this is *not* restricted to Gaussian smearing: all smearing schemes are controlled by the `degauss` parameter, and when this parameter is not set, the error occurs.

4.2.7 Error in routine splitwf (36197): wrong size for pwt

Usually this occurs when pw2bgw is redone (pw2bgw deletes intermediate files, making another pw2bgw run impossible). This also appears in cases similar to Section 4.2.2. A complete bands-pw2bgw run has to be redone.

4.2.8 Error in routine PW2BGW(19):input pw2bow

Usually this occurs when something else happens between a bands run and a pw2bgw run for it. A complete bands-pw2bgw run has to be redone.

4.3 Trouble shooting in epsilon and sigma

4.3.1 Selected number of bands breaks degenerate subspace.

Run degeneracy_check.x WFN to see degeneracy-allowed number of bands. This error occurs when one band in a degeneracy subspace is considered but others are not. Also, the band_index_min and band_index_max parameters shouldn't be too close to vxc_diag_min and vxc_diag_max, or the error occurs.

4.3.2 WFN ifmin/ifmax fields are inconsistent

The full message is

```

WFN ifmin/ifmax fields are inconsistent:
- there is a valence state above the middle energy
- there is a conduction state below the middle energy
Possible causes are:
(1) Your k-point sampling is too coarse and cannot resolve the Fermi energy.
    Try to carefully inspect your mean-field energies, and consider using a
    ↪ finer
    k-grid.
(2) You are using eqp.dat and the QP corrections change the character of some
    ↪ s
    tates
    from valence<->conduction. In this case, you should use another mean-field
    ↪ the
    ory
    that gives the same ground state as your GW calculation.
(3) You are running inteqp, but you are either shifting the Fermi energy or
    ↪ usi
    ng
    restricted transformation.

```

The direct causes of this error are already listed above. But it takes some time to see what is the deeper reason, and how to solve it:

- Sometimes when the occupation option in the 2.1-wfn and 2.2-wfnq steps is not correct. If fixed is used for a metal, for example, some positions that should be a part of a hole Fermi pocket are occupied by electrons, and therefore the highest occupied state has higher energy than the lowest unoccupied state. This usually means the smearing scheme needs to be changed.
- When you shift the occupation in a WFN file (Section 4.6.6), but forget to change the ifmax dataset correspondingly, this error will also occur, regardless of how you change the eqp.dat.

4.3.3 Segmentation fault: address not mapped to object at address

The root of this error differs from case to case.

If we see

```

q-pt      2: Head of Epsilon      =   NaN      NaN
q-pt      2: Epsilon(2,2)         =   NaN      NaN

```

usually this means a “divided-by-zero” error occurs. This may occur when we incorrectly use the insulator procedure to calculate a metallic system (as long as DFT thinks the system is metallic, the error has the potential to occur, regardless of whether the system is metallic after *GW* correction), often regardless of the smearing type.

4.3.4 eqpcor mean-field energy mismatch

This error happens when we try to do an eigenvalue self-consistent calculation, and `epsilon` finds the DFT energies given in `eqp.dat` are different from the energies in `WFN`. This sometimes is a technical problem (the Rydberg energy definitions used in QuantumESPRESSO and BerkeleyGW are slightly different), and can be solved by increasing `TOL_eqp` in the source code of BerkeleyGW. The error may also be reported when the DFT energies in `eqp.dat` are mistakenly changed (we should only change the column corresponding to the corrected energy).

4.3.5 ERROR: occupations (ifmax field) inconsistent between WFN and WFNq files.

```
ERROR: occupations (ifmax) inconsistent between WFN and WFNq files.
Remember that you should NOT use WFNq for metals and graphene.
```

4.3.6 ERROR: Unexpected characters were found while reading the value for the keyword

This usually happens when the input file contains a line like

```
number_bands = 148
```

while the correct format is

```
number_bands 148
```

4.3.7 forrtl: severe (24): end-of-file during read, unit -5, file Internal List-Directed Read

This usually happens when we should write `qpoints` but actually write `kpoints` (or the opposite).

4.3.8 ERROR: Inconsistent screening, truncation, or q0 vector

The full error message may be

```
ERROR: the input truncation flag indicates that the Coloumb interaction v(q0)
diverges for q0->0. However, you have q0 exactly zero.
You should always specify a *nonzero* q0->0 vector unless you have 0D
truncation, i.e., spherical or box truncation.
```

```
ERROR: Inconsistent screening, truncation, or q0 vector
```

This arises when we are dealing with a metal but forget to add `screening_metal` to `sigma.inp`.

```
ERROR: cannot use metallic screening with q0 = 0.
You should either specify a nonzero q0->0 vector or use another screening
↪ flag.
```

4.3.9 cannot use metallic screening with q=0

As the name implies, when doing a metallic calculation, we need to make sure that the $\mathbf{q} \rightarrow 0$ point is the smallest *non-zero* point in the dense \mathbf{k} -grid (Section 3.1.4).

4.3.10 ERROR: genwf mpi: No match for rkq point

4.3.11 ERROR: Missing bands in file eqp_co.dat

This happens when doing `inteqp`. The origin of the error is just its name implies. Note that this error sometimes occurs for unnoticed reasons:

- When the pseudopotential is changed, the number of bands may change, because the orbitals included in the pseudopotentials change. Now if `band_index_max` and `band_index_min` are set according to the old pseudopotentials, and the Fermi energy happens to fall outside of the range between the two, the error occurs.

4.3.12 forrtl: severe (71): integer divide by zero

If this happens after `Calculation parameters:`, it may arise from mistakenly setting `band_index_max` to a value smaller than `band_index_min`. In this case, the number of bands considered will be zero, and thus a divide-by-zero error occurs when `sigma.x` tries to distribute computational loads.

4.4 Trouble shooting in wannier90

4.4.1 w90_wannier90_readwrite_read: mismatch in WTe2.eig

When reading a `.eig` file, `wannier90` doesn't really look at the band index and k -point index. Rather, it completely relies on `num_bands` and `mp_grid`. Thus, if the number of `nbnd` in the QuantumESPRESSO run – which decides the number of bands in the `.eig` file – isn't `num_bands`, `wannier90` finds bands in the `.eig` file messed up, and the error occurs.

4.4.2 WTe2.amn has not the right number of bands

4.5 Trouble shooting in kernel and absorption

4.5.1 ERROR: Inconsistent symmetry treatment of the fine and shifted grids with the momentum operator

4.6 Checklist for unexpected results

Sometimes the calculation ends successfully, but the result seems strange. Below are some checklists.

4.6.1 Band symmetry higher than the space group shown at the beginning of `bands.out`

- Usually this is because of an approximate symmetry, which is ignored by QuantumESPRESSO because its tolerance is very low.
- Are all steps in the DFT calculation using the same crystal structure?

4.6.2 Band structure looks very far from the literature

- Check the crystal structure: if it comes from relaxation, does it converges?
- For 2D materials, when we change the vacuum distance and use crystal coordinates for atomic positions at the same time, always double check whether we scale the atomic positions correctly. The formula is

$$\text{new } z \text{ coordinate} = \frac{\text{old vacuum distance}}{\text{new vacuum distance}} \times \text{old } z \text{ coordinate.} \quad (4.1)$$

- Are all steps in the DFT calculation using the same crystal structure?
- Is the Fermi energy correct? Sometimes we change the band structure but forget to change the Fermi energy used to plot bands.

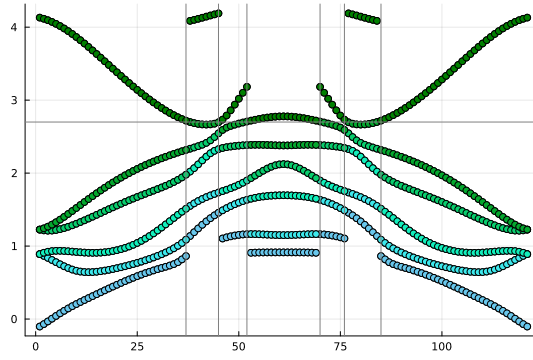


Figure 4.1: Example of how `inteqp` misidentifies DFT-level bands: the data is from the DFT column of `eqp.dat`; the colors of points are about the band index.

4.6.3 Band plot is empty

- Are there enough bands? If `nbnd` is not set for an insulator, no conduction band will be considered.
- Is the Fermi energy correct? If the Fermi energy is set too high (which may come from, say, wrong unit), then naturally there is no band in the plot.

4.6.4 Band plot is not continuous

TODO: it's k -points that are shuffled, or the band indices, or both???

If the system is metallic in the DFT level (regardless of what GW says about the material, and the screening model used) and `inteqp` is used, this is expected: somehow, `inteqp` assumes the system is an insulator, and thus states above the Fermi energy (but not too far from it) has to be in one band. Thus, if, say, the 120th band has more than one intersection points with the Fermi energy level, its part below φ_F will be recognized as the 119th band in the eyes of `inteqp`. This can be seen by plotting the DFT column of the `eqp.dat` output of `inteqp` (Figure 4.1).

4.6.5 The size of band gap

DFT is infamous for underestimating the band gap.

- Use hybrid functionals like HSE.
- Let GW correct the band structure. TODO: but how? How to avoid the error in Section 4.3.2?

4.6.6 When we get a semimetal in the DFT step but it should be an insulator

This is similar to Section 4.6.5.

Note that naively feeding the semimetal result into BerkeleyGW while still using the insulator procedure may result in errors in Section 4.3.3.

One way to solve the problem is to manually move the conduction bands and the valence bands away from each other. Naively using the `eqp_correction` option and shifting bands near the Fermi surface away from each other leads to Section 4.3.2, precisely because “QP corrections” (i.e. the energy shift manually added by me) change the character of some states from valence to conduction. The `mf_header/kpoints/occ` and `mf_header/kpoints/ifmax` datasets in the `WFN.h5` file have to be modified accordingly. TODO: should this be done in 2-sigma?

The problem with this method is we don't have `eqp_correction` in `kernel`. TODO

Bibliography

- [1] Irene Aguilera, Christoph Friedrich, Gustav Bihlmayer, and Stefan Blügel. G w study of topological insulators bi 2 se 3, bi 2 te 3, and sb 2 te 3: Beyond the perturbative one-shot approach. *Physical Review B*, 88(4):045206, 2013.
- [2] Bradford A Barker, Jack Deslippe, Johannes Lischner, Manish Jain, Oleg V Yazyev, David A Strubbe, and Steven G Louie. Spinor g w/bethe-salpeter calculations in berkeleygw: Implementation, symmetries, benchmarking, and performance. *Physical Review B*, 106(11):115127, 2022.
- [3] Christian Brouder, Gianluca Panati, Matteo Calandra, Christophe Mourougane, and Nicola Marzari. Exponential localization of wannier functions in insulators. *Physical review letters*, 98(4):046402, 2007.
- [4] Mauro Del Ben, H Felipe, Andrew Canning, Nathan Wichmann, Karthik Raman, Ruchira Sasanka, Chao Yang, Steven G Louie, and Jack Deslippe. Large-scale gw calculations on pre-exascale hpc systems. *Computer Physics Communications*, 235:187–195, 2019.
- [5] Jack Deslippe, Georgy Samsonidze, David A. Strubbe, Manish Jain, Marvin L. Cohen, and Steven G. Louie. Berkeleygw: A massively parallel computer package for the calculation of the quasiparticle and optical properties of materials and nanostructures. *Computer Physics Communications*, 183(6):1269–1289, 2012.
- [6] Sergey V Faleev, Mark Van Schilfgaarde, and Takao Kotani. All-electron self-consistent g w approximation: Application to si, mno, and nio. *Physical review letters*, 93(12):126406, 2004.
- [7] Mark S Hybertsen and Steven G Louie. Electron correlation in semiconductors and insulators: Band gaps and quasiparticle energies. *Physical Review B*, 34(8):5390, 1986.
- [8] Nicola Marzari, Arash A Mostofi, Jonathan R Yates, Ivo Souza, and David Vanderbilt. Maximally localized wannier functions: Theory and applications. *Reviews of Modern Physics*, 84(4):1419, 2012.
- [9] John P Perdew, Robert G Parr, Mel Levy, and Jose L Balduz Jr. Density-functional theory for fractional particle number: derivative discontinuities of the energy. *Physical Review Letters*, 49(23):1691, 1982.
- [10] Bi-Ching Shih, Yu Xue, Peihong Zhang, Marvin L Cohen, and Steven G Louie. Quasiparticle band gap of zno: High accuracy from the conventional g 0 w 0 approach. *Physical review letters*, 105(14):146401, 2010.
- [11] M. Shishkin, M. Marsman, and G. Kresse. Accurate quasiparticle spectra from self-consistent gw calculations with vertex corrections. *Phys. Rev. Lett.*, 99:246403, Dec 2007.